# Effect of Injection Velocity on Heat Transfer of Water/Alumina Nano Fluid in A Rectangular Microchannel

**Afshin Ahmadi Nadooshan** *
Department of Mechanical Engineering,
Shahrekord University, Shahrekord, Iran
E-mail: ahmadi@sku.ac.ir
*Corresponding author

**Afshin Shiriny**
Department of Mechanical Engineering,
Shahrekord University, Shahrekord, Iran
E-mail: shiriny@yahoo.com

**Morteza Bayareh**
Department of Mechanical Engineering,
Shahrekord University, Shahrekord, Iran
E-mail: m.bayareh@sku.ac.ir

**Received: 6 November 2019, Revised: 28 February 2020, Accepted: 9 March 2020**

**Abstract:** In this study, forced convection heat transfer of water/alumina Nano fluid in a rectangular microchannel with cross-flow injection is studied. The Nano fluid enters the microchannel with a temperature of 293 K and cools its walls. The upper wall of the microchannel is at constant temperature of 303 K. On the lower wall, there are two holes for injection of Nano fluid flow. Other parts of the microchannel wall are insulated. Slip velocity boundary condition is used for the walls of the microchannel. Simulations are performed for different injection velocities and the results are presented as velocity and temperature fields, and variation of the Nusselt number. The results show that the slip velocity on the channel wall and the Nusselt number increase by increasing the injection velocity. It is revealed that the Nusselt number is maximum at the channel entrance and decreases along the channel. After each injection, local Nusselt number increases due to the increase of the temperature gradient in the microchannel. Moreover, an optimal value for the ratio of the injection velocity to the inlet velocity is achieved using performance evaluation criteria (PEC). It is concluded that $v_{inj}/u_c = 10$ is an optimal value of the injection velocity, leading to maximum PEC.

**Keywords:** Forced Convection, Microchannel, Nano Fluid, Slip Velocity, Vertical Injection

**Reference:** Afshin Ahmadi Nadooshan, Afshin Shiriny, and Morteza Bayareh, "Effect of Injection Velocity on Heat Transfer of Water/Alumina Nano Fluid in A Rectangular Microchannel", Int J of Advanced Design and Manufacturing Technology, Vol. 13/No. 2, 2020, pp. 41–49.

**Biographical notes: Afshin Ahmadi Nadooshan** is now an Associate Professor at the Faculty of Engineering, Shahrekord University since 2017. His current research interest includes numerical simulation, energy saving and two phase flow. **Afshin Shiriny** received his MSc in Mechanical Engineering (Energy Conversion) from Shahrekord University in 2020. **Morteza Bayareh** is now an Associate Professor at the Faculty of Engineering, Shahrekord University since 2019.

## 1 INTRODUCTION

In recent years, microchannels have been used for heat rejection in various engineering applications, including medical applications, ink jet printers, and micro electromechanical systems [1-2]. The use of nanoparticles as a coolant fluid has attracted the researchers due to the increase in the heat transfer coefficient. Nano fluids are suspensions of nanoparticles or carbon nanotubes in base fluids such as water, ethylene glycol and oil. They play an essential role in heating and cooling processes. The name of the Nano fluid was first proposed by Choi [3] to characterize a mixture of nanoparticles dispersed within the base fluid. Adding nanoparticles to base fluid usually results in an increase in the viscosity.

Akbarinia et al. [4] investigated forced convection of water/alumina Nano fluid in a two-dimensional microchannel and demonstrated that viscosity increases with the volume fraction of nanoparticles ($\varphi$). Many studies have been carried out to evaluate the thermal conductivity of nanoparticles relative to the base fluids [5-14]. For example, Kamali et al. [15] investigated forced convection heat transfer of water/copper Nano fluid in a micro-tube under constant heat flux boundary condition numerically. Their results showed that the heat transfer coefficient and Nusselt number (Nu) are increased compared to the base fluid. Several studies have shown that Nu and heat transfer increase with the Reynolds number (Re) and $\varphi$ [16-23].

In addition, the decrease in the diameter of the solid nanoparticles due to an increase in the effective surface and the uniform distribution of particles along the channel leads to an increase in Nu [24-26]. Investigations showed that slip velocity and Nu increase with the magnetic field intensity [27-29]. In thermal channels, the fluid temperature near the hot surfaces is always higher than that of the channel center. Thus, if low temperature fluid can be mixed with the hot one adjacent to the target surface, the heat transfer rate increases considerably. For this purpose, various techniques such as injecting fluid jets, suction and blasting have been used in areas close to the target surface. Nano fuids have been used as a cooling fluid to improve heat transfer in most of the studies conducted in this field.

Jha and Aina [30] studied the hydrodynamic and thermal behavior of the fully developed flow in vertical microchannel with porous medium considering the slip velocity and temperature jump on the channel walls in the presence of injection and suction. They found that as the injection velocity increases, volume flow rate increases and the heat transfer decreases. Furthermore, the possibility of the occurrence of reverse flow on the cold wall decreases with the Knudsen number.

Lopez et al. [31] investigated the heat transfer and entropy generation of water/alumina Nano fluid in a porous microchannel by considering the effect of injection, slip velocity and radiation heat transfer. They found that Nu increases on the hot wall and decreases on the cold wall by increasing $\varphi$ and injection velocity.

In the present study, forced convection heat transfer of water/alumina Nano fluid flow in a rectangular microchannel is simulated, while the Nano fluid flow is injected vertically through two holes on the lower wall. The effect of injection velocity on heat transfer is investigated and its optimal value is determined using PEC. The main objective of the present paper is to provide the optimal value of injection velocity in a microchannel in the presence of a Nano fluid.

## 2 PROBLEM STATEMENT

A two-dimensional and horizontal rectangular microchannel with length L and height H is considered as shown in “Fig. 1”.

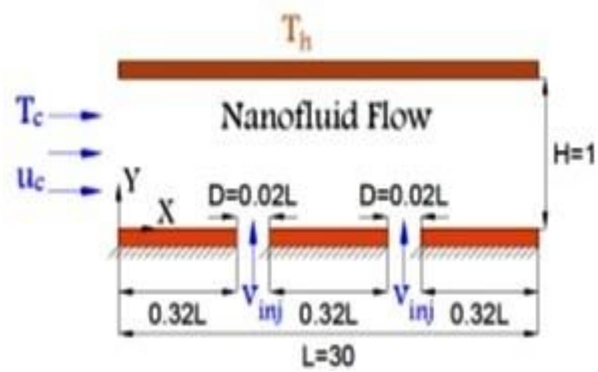


**Fig. 1** Schematic of the problem.

The water/alumina Nano fluid flow enters the microchannel with velocity of $u_c$ and temperature of $T_c$ = 293 K and exits after cooling the walls of the microchannel. The upper wall temperature is equal to $T_h$ = 303 K and the lower wall is insulated. On the lower wall, two holes of diameter d = 6 μm are embedded through which the Nano fluid flow is injected into the microchannel with the velocity $v_{inj}$. The flow inside the microchannel is considered as steady and laminar and the fluid is assumed to be Newtonian. The slip velocity boundary condition is imposed on the upper and lower walls of the microchannel and the temperature jump is ignored. The thermophysical properties of the Nano fluid are presented in “Table 1”. The Reynolds number of the inlet flow is considered to be Re = 1. In this study, the slip length on the microchannel walls is $\beta$ = 0.1 μm and $\varphi$ = 2%.

**Table 1** Thermophysical properties of water/alumina Nano fluid [32]

| $\phi$ (%) | $\rho_{nf}$ $(kg/m^3)$ | $\mu_{nf}$ $(Pa.s)$ | $k_{nf}$ $(W/m.K)$ | $(c_p)_{nf}$ $(J/kg.K)$ |
|---|---|---|---|---|
| 0 | 997.1 | $8.91\times10^{-4}$ | 4179 | 0.613 |
| 2 | 1056.5 | $9.37\times10^{-4}$ | 3922.4 | 0.653 |
| 4 | 1116 | $9.87\times10^{-4}$ | 3693.3 | 0.695 |

## 3 GOVERNING EQUATIONS

The governing equations for steady and laminar Nano fluid flow are as follows:

Continuity equation:

$$\frac{\partial u}{\partial x}+\frac{\partial v}{\partial y}=0 \quad (1)$$

Momentum equation in x-direction:

$$u\,\partial u/\partial x + v\,\partial u/\partial y = -1/\rho\_nf\ \ \partial p/\partial x + \mu\_nf/\rho\_nf\ \ ((\partial\text{^}2\,u)/(\partial x\text{^}2\,) + (\partial\text{^}2\,u)/(\partial y\text{^}2\,)) \quad (2)$$

Momentum equation in y-direction:

$$u\frac{\partial v}{\partial x}+v\frac{\partial v}{\partial y}=-\frac{1}{\rho_{nf}}\frac{\partial p}{\partial y}+\frac{\mu_{nf}}{\rho_{nf}}\left(\frac{\partial^2 v}{\partial x^2}+\frac{\partial^2 v}{\partial y^2}\right) \quad (3)$$

Energy equation:

$$u\frac{\partial T}{\partial x}+v\frac{\partial T}{\partial y}=\alpha_{nf}\left(\frac{\partial^2 T}{\partial x^2}+\frac{\partial^2 T}{\partial y^2}\right) \quad (4)$$

Boundary conditions are as follows:

| | |
|---|---|
| $u=u_c\ ,v=0\ ,T=T_c$ | For $x=0\ ,\ 0\le y\le h$ |
| $\frac{\partial u}{\partial x}=0\ ,v=0\ ,\frac{\partial T}{\partial x}=0$ | For $x=0\ ,\ 0\le y\le h$ |
| $u=u_s\ ,v=0\ ,\frac{\partial T}{\partial y}=0$ | For $0\le x\le l\ ,\ y=0$ |
| $u=u_s\ ,v=0\ ,T=T_h$ | For $0\le x\le l\ ,\ y=h$ |

Where, $u_s$ is slip velocity on upper and lower walls and defined as follows:

$$u_s=\pm\beta\left(\frac{\partial u}{\partial y}\right)_{y=0,h} \quad (5)$$

Moreover, $\beta$ is slip coefficient and the positive and negative signs correspond to lower and upper walls, respectively. Using the following non-dimensional parameters, the governing equations and boundary conditions are non-dimensionalized.

$$X=\frac{x}{h}\ ,\quad Y=\frac{y}{h}\ ,\quad U=\frac{u}{u_c}\ ,\quad V=\frac{v}{u_c}\ ,\quad B=\frac{\beta}{h}$$
$$\boldsymbol{\theta}=\frac{T-T_c}{T_h-T_c}\ ,P=\frac{p}{\rho_{nf}{u_c}^2},Re=\frac{u_c h}{\vartheta_f},Pr=\frac{\vartheta_f}{\alpha_f} \quad (6)$$

Hence, dimensionless governing equations are:

$$\frac{\partial U}{\partial X}+\frac{\partial V}{\partial Y}=0 \quad (7)$$

$$U\frac{\partial U}{\partial X}+V\frac{\partial U}{\partial Y}=-\frac{\partial P}{\partial X}+\frac{\vartheta_{nf}}{\vartheta_f Re}\left(\frac{\partial^2 U}{\partial X^2}+\frac{\partial^2 U}{\partial Y^2}\right) \quad (8)$$

$$U\frac{\partial V}{\partial X}+V\frac{\partial V}{\partial Y}=-\frac{\partial P}{\partial Y}+\frac{\vartheta_{nf}}{\vartheta_f Re}\left(\frac{\partial^2 V}{\partial X^2}+\frac{\partial^2 V}{\partial Y^2}\right) \quad (9)$$

$$U\frac{\partial \theta}{\partial X}+Y\frac{\partial \theta}{\partial Y}=\frac{\alpha_{nf}}{\alpha_f Re.Pr}\left(\frac{\partial^2 \theta}{\partial X^2}+\frac{\partial^2 \theta}{\partial Y^2}\right) \quad (10)$$

In addition, non-dimensional governing boundary conditions are as follows:

| | |
|---|---|
| $U=1\ ,V=0\ ,\theta=0$ | For $X=0\ ,\ 0\le Y\le 1$ |
| $\frac{\partial U}{\partial X}=0\ ,V=0\ ,\frac{\partial \theta}{\partial X}=0$ | For $X=\frac{l}{h}\ ,\ 0\le Y\le 1$ |
| $U=U_s\ ,V=0\ ,\frac{\partial \theta}{\partial Y}=0$ | For $0\le X\le\frac{l}{h}\ ,\ Y=0$ |
| $U=U_s\ ,V=0\ ,\theta=1$ | For $0\le X\le\frac{l}{h}\ ,\ Y=1$ |

Where dimensionless slip velocity is defined as follows:

$$U_s=\pm B\left(\frac{\partial U}{\partial Y}\right)_{Y=0,1} \quad (11)$$

The density of Nano fluid is calculated using the following relation [33]:

$$\rho_{nf} = (1-\phi)\rho_f + \phi\rho_s \tag{12}$$

Thermal diffusion coefficient of Nano fluid is defined as:

$$\alpha_{nf} = \frac{k_{nf}}{(\rho c_p)_{nf}} \tag{13}$$

Specific heat capacity of Nano fluid is calculated using bongrino relation [34]:

$$(\rho c_p)_{nf} = (1-\varphi)(\rho c_p)_f + \varphi(\rho c_p)_s \tag{14}$$

Viscosity and thermal conductivity of nanofluid are obtained using Brinkman [35] and Patel et al. [34] relations, respectively:

$$\mu_{nf} = \frac{\mu_f}{(1-\phi)^{0.25}} \tag{15}$$

$$k_{nf} = k_f\left(1 + \frac{k_s A_s}{k_f A_f} + cP_e\frac{k_s A_s}{k_f A_f}\right) \tag{16}$$

Where, c = 25000 is an experimental constant. $k_f = 0.613$ W/mK is thermal conductivity of the base fluid and $k_s = 40$ W/mK is that of nanoparticles. The ratio of molecular of the base fluid to that of solid nanoparticles is defined as follows [32]:

$$\frac{A_f}{A_s} = \frac{d_f}{d_s}\left(\frac{\varphi}{1-\varphi}\right) \tag{17}$$

In addition, $P_e$ is defined as follows:

$$P_e = \frac{u_s d_s}{\alpha_f} \tag{18}$$

$u_s$ is related to the effect of the Brownian motion and is calculated as follows:

$$u_s = \frac{2K_b T}{\pi\mu_f d_s^2} \tag{19}$$

Where, $K_b = 1.3807 \times 10^{-23}$ J/K is the Boltzmann constant. The molecular diameter of water and solid nanoparticles is $d_f = 2$ A° and $d_s = 40$ nm, respectively ([36]).

The local Nusselt number ($Nu_x$) is:

$$Nu_x = -\frac{k_{nf}}{k_f}\left(\frac{\partial\theta}{\partial Y}\right)_{Y=1} \tag{20}$$

The average Nusselt number ($Nu_m$) is:

$$Nu_m = \frac{1}{L}\int_0^L Nu_x dX \tag{21}$$

Performance evaluation criteria (PEC) for lower wall is defined as follows [29]:

$$PEC = \frac{\left(\frac{Nu}{Nu_i}\right)}{\left(\frac{\Delta P}{\Delta P_i}\right)^{1/3}} \qquad [22]$$

Where, ΔP is the microchannel pressure drop and the subscript *i* is related to the absence of flow injection from the lower microchannel wall.

## 4 GRID STUDY

The values of dimensionless temperature and dimensionless velocity on the point (l/2, l/2) for Re = 1 for the injection flow are shown in “Table 2” on various grid resolutions. The grid resolutions of 60×600 and 70×700 lead to similar results approximately. Hence, the grid resolution of 60×600 is selected for further simulations.

**Table 2** Dimensionless temperature and dimensionless velocity on the point (l/2, l/2) for various grid resolutions at Re = 1

| | 50 × 500 | 60 × 600 | 70 × 700 |
|---|---|---|---|
| $\theta$ | 0.8825 | 0.8824 | 0.8824 |
| $U$ | 2.102 | 2.103 | 2.103 |

## 5 VALIDATION

The validation of this study has been carried out with the results of Jalali and Karimipour [32] who investigated the effect of vertical injection on the channel wall. The dimensionless velocity profile at the vertical line X = 0.6L is plotted in “Fig. 2”, for input Reynolds number of Re = 10, φ = 0.02 and the slip coefficient of B = 0.1, and injection Reynolds number of 1. Moreover, in “Fig. 3”, the variation of $Nu_x$ along the microchannel wall are compared with the reference results for input and injection Reynolds numbers of Re = 100, B = 0.1 and ∅ = 0.02. The present results are in excellent agreement with those of Jalali and Karimipour [32].

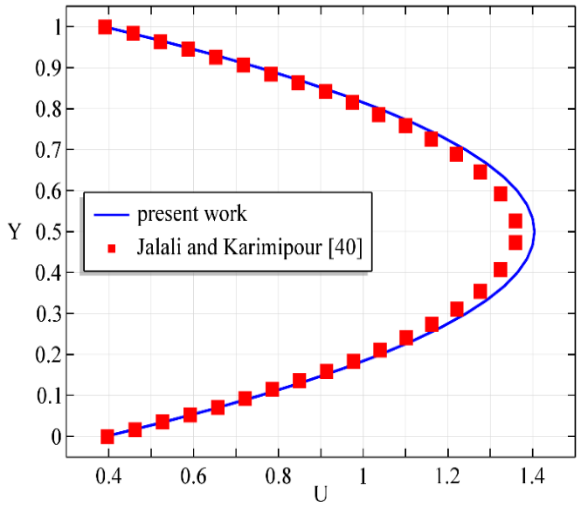


**Fig. 2** Dimensionless velocity profile at the vertical line X = 0.6L for input Reynolds number Re = 10, ∅ = 0.02, B = 0.1, and injection Reynolds number of 1.

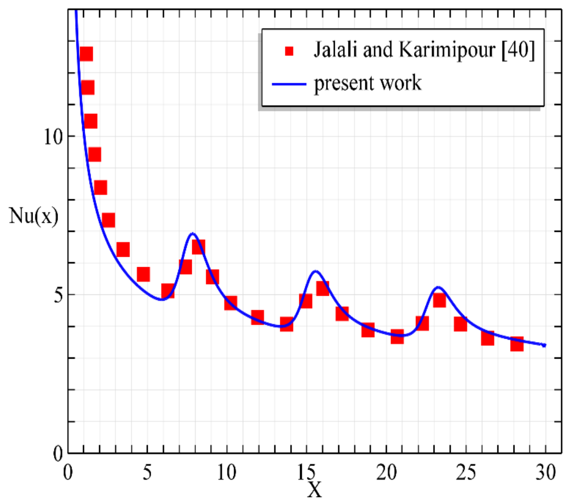


**Fig. 3** $Nu_x$ for input and injection Reynolds numbers of 100, ∅ = 0.02, and B = 0.1.

## 6 RESULTS

Forced convection heat transfer of the water/alumina Nano fluid in a rectangular microchannel is numerically investigated as shown in "Fig. 1". The present simulations are carried out for various injection velocities on the lower wall of the microchannel. Figures 4 and 5 show dimensionless velocity and dimensionless temperature profiles for Nano fluid flow along the vertical line X = 0.5L at the input Reynolds number Re = 1, ∅ = 0.02 and B = 0.1 for different injection velocities. It is observed that the velocity distribution is parabolic and fully developed. It is not zero on the walls of the microchannel due to the slip boundary condition. The maximum velocity occurs at the channel center. In addition, the velocity and maximum velocity increase at the cross-section of the microchannel by increasing the injection velocity. This is confirmed by continuity governing equation.

In the case of the dimensionless temperature profile, as shown in "Fig. 5", the temperature is higher in the vicinity of the hot wall.

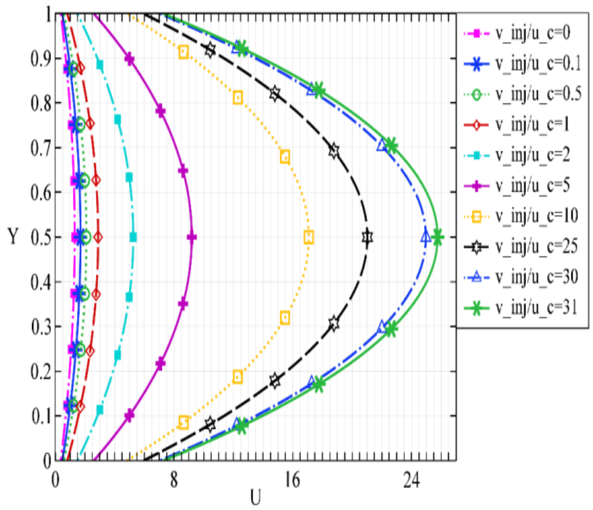


**Fig. 4** Dimensionless velocity profile at the vertical line X = 0.5L for input Reynolds number Re = 1, ∅ = 0.02, B = 0.1, and different injection velocities.

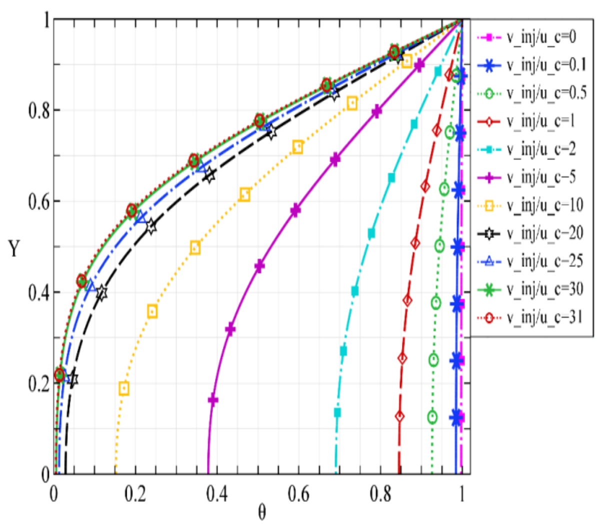


**Fig. 5** Dimensionless temperature profile at the vertical line X = 0.5L for input Reynolds number Re = 1, ∅ = 0.02, B = 0.1, and different injection velocities.

It decreases with the injection velocity due to low temperature of the input flow to the microchannel. It is also shown in "Fig. 6" that the dimensionless temperature decreases along the microchannel after each injection.

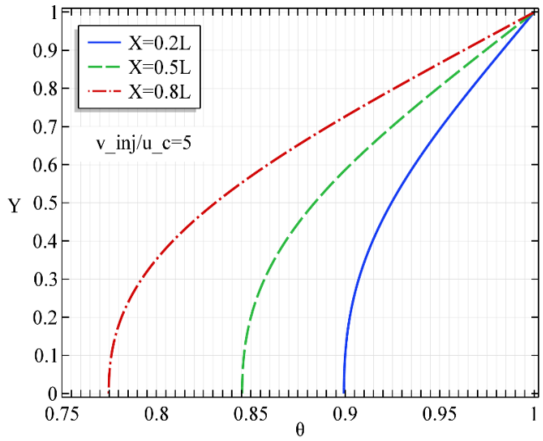


**Fig. 6** Dimensionless temperature profile for $v_{inj}/u_c = 5$.

Figure 7 illustrates the effect of different values of the injection velocity on the non-dimensional microchannel slip velocity for input Reynolds number Re = 1, ∅ = 0.02 and B = 0.1. As can be seen, the slip velocity initially decreases along the microchannel wall. After each injection, it increases to eventually reach a constant amount at the microchannel outlet. As the injection velocity increases, the slip velocity increases.

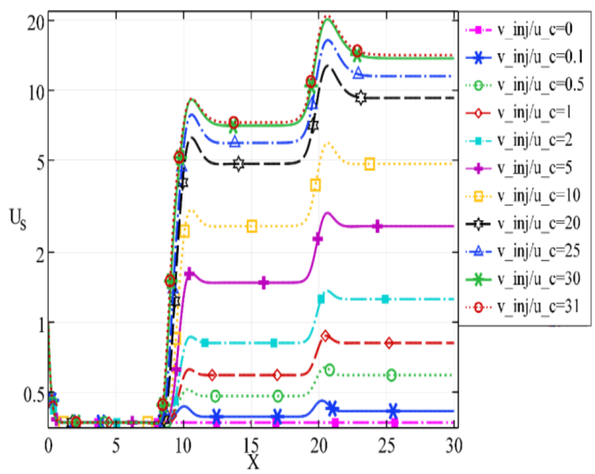


**Fig. 7** Dimensionless slip velocity at the upper wall for input Reynolds number Re = 1, ∅ = 0.02, B = 0.1, and different injection velocities.

Effect of injection velocity on $Nu_x$ is shown in "Fig. 8" for Re=1, ∅ =0.02 and B=0.1. It is found that Nu increases as the injection velocity increases. At the microchannel entrance, Nu is maximum due to the difference in the temperature between the Nano fluid and the microchannel wall, and then, Nu decreases by decreasing the temperature gradient along the microchannel. After each injection on the lower wall, an increase in Nu is observed. It is due to an increase in the nanofluid temperature gradient. The variations of $Nu_m$ for various injection velocities are also shown in "Fig. 9". As mentioned above, the temperature gradient and $Nu_m$ increase with injection velocity.

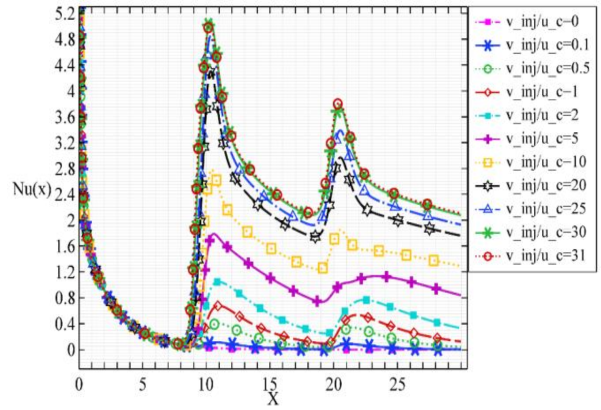


**Fig. 8** $Nu_x$ calculated on the upper wall for input Reynolds number Re = 1, ∅ = 0.02, B = 0.1, and different injection velocities.

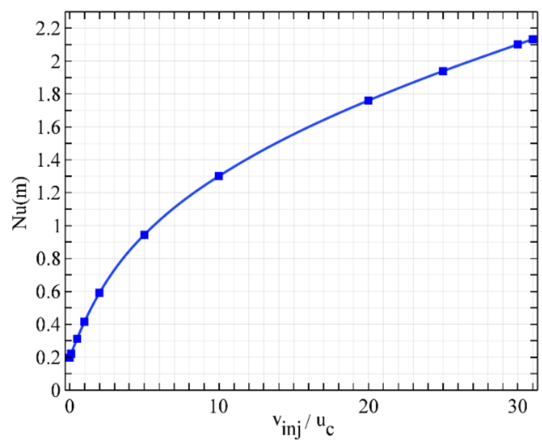


**Fig. 9** $Nu_m$ calculated on the upper wall for input Reynolds number Re = 1, ∅ = 0.02, B = 0.1, and different injection velocities.

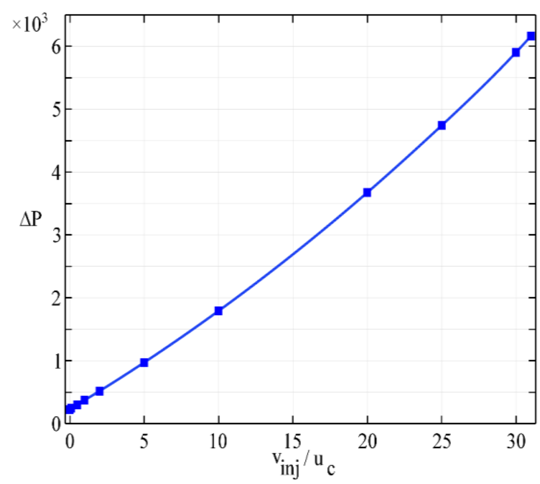


**Fig. 10** Pressure drop for input Reynolds number Re = 1, ∅ = 0.02, B = 0.1, and different injection velocities.

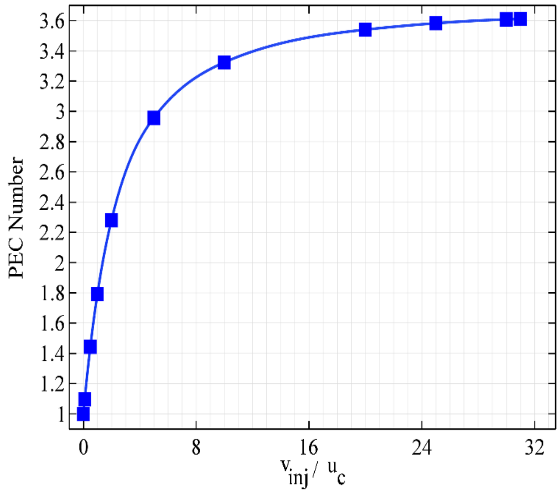


**Fig. 11** PEC variation for input Reynolds number Re = 1, ∅ = 0.02, B = 0.1, and different injection velocities.

In "Fig. 10", variations of the pressure drop of nanofluid are plotted for different injection velocities. As the injection velocity increases, the pressure drop increases. Figure 11 shows the PEC for Re = 1, ∅ = 0.02 and B = 0.1 and various dimensionless injection velocities. The figure demonstrates that the changes in the PEC number are not considerable with the increase in the dimensionless injection velocity greater than 30. It can be concluded that $v_{inj}/u_c = 10$ is an optimal value of the injection velocity, leading to maximum PEC (or maximum heat transfer rate).

## 7 CONCLUSION

Forced convection of water/alumina Nano fluid in a rectangular microchannel with an aspect ratio of AR = 30 was numerically simulated. The slip coefficient of the walls was B = 0.1 and two holes were inserted at the bottom wall of the microchannel to inject the Nano fluid. The effect of injection velocity on velocity and temperature distributions was investigated. The following results were obtained:

- The slip velocity is maximum at the channel inlet and increases along the channel by each injection. It ultimately reaches a constant value at the channel outlet. Slip velocity increases with the injection velocity.
- Nu is maximum at the channel entrance and decreases along the channel. After each injection, $Nu_x$ increases due to the increase of the temperature gradient in the microchannel.
- The pressure drop and $Nu_m$ increase with the injection velocity.
- The maximum heat transfer rate occurs for $v_{inj}/u_c = 10$. There is no significant change in the PEC by further increasing.

## 8 CONFLICT OF INTEREST

On behalf of all authors, the corresponding author states that there is no conflict of interest.

## ACKNOWLEDGMENTS

This research was financially supported by Shahrekord University.

## REFERENCES

[1] Malvandi, A., Ganji, D. D., Effects of Nanoparticle Migration and Asymmetric Heating On Magnetohydrodynamic Forced Convection of Alumina/Water Nanofluid in Microchannels, European Journal of Mechanics-B/Fluids, Vol. 52, 2015, pp. 169-184.

[2] Mokrani, O., Bourouga, B., Castelain, C., and Peerhossaini, H., Fluid Flow and Convective Heat Transfer in Flat Microchannels, International Journal of Heat and Mass Transfer, Vol. 52, No. 5-6, 2009, pp. 1337-1352.

[3] Choi, S. U. S., Singer, D. A., and Wang, H. P., Developments and Applications of Non-Newtonian Flows, Asme Fed, Vol. 66, 1995, pp. 99-105.

[4] Akbarinia, A., Abdolzadeh, M., and Laur, R., Critical Investigation of Heat Transfer Enhancement Using Nanofluids in Microchannels with Slip and Non-Slip Flow Regimes, Applied Thermal Engineering, Vol. 31, No. 4, 2011, pp. 556-565.

[5] Bhattacharya, P., Samanta, A. N., and Chakraborty, S., Numerical study of Conjugate Heat Transfer in Rectangular Microchannel Heat Sink with Al2O3/H2O Nano Fluid, Heat and Mass Transfer, Vol. 45, No. 10, 2009, pp. 1323-1333.

[6] Devendiran, D. K., Amirtham, V. A., A Review On Preparation, Characterization, Properties and Applications of Nano Fluids, Renewable and Sustainable Energy Reviews, Vol. 60, 2016, pp. 21-40.

[7] Duangthongsuk, W., Wongwises, S., Measurement of Temperature-Dependent Thermal Conductivity and Viscosity of TiO2-Water Nano Fluids, Experimental Thermal and Fluid Science, Vol. 33, No. 4, 2009, pp. 706-714.

[8] Ho, C. J., Wei, L. C., and Li, Z. W., An Experimental Investigation of Forced Convective Cooling Performance of a Microchannel Heat Sink with Al2O3/Water Nano Fluid. Applied Thermal Engineering, Vol. 30, No. 2-3, 2010, pp. 96-103.

[9] Lee, J., Mudawar, I., Assessment of the Effectiveness of Nano Fluids for Single-Phase and Two-Phase Heat Transfer in Micro-Channels, International Journal of Heat and Mass Transfer, Vol. 50, No. 3-4, 2007, pp. 452-463.

[10] Masuda, H., Ebata, A., and Teramae, K., Alteration of Thermal Conductivity and Viscosity of Liquid by Dispersing Ultra-Fine Particles, Dispersion of Al2O3, SiO2 and TiO2 Ultra-Fine Particles, 1993.

[11] Mintsa, H. A., Roy, G., Nguyen, C. T., and Doucet, D., New Temperature Dependent Thermal Conductivity Data for Water-Based Nano Fluids, International Journal of Thermal sciences, Vol. 48, No. 2, 2009, pp. 363-371.

[12] Reddy, M. C. S., Rao, V. V., Experimental Studies On Thermal Conductivity of Blends of Ethylene Glycol-Water-Based TiO2 Nano Fluids, International Communications in Heat and Mass Transfer, Vol. 46, 2013, pp. 31-36.

[13] Santra, A. K., Sen, S., and Chakraborty, N., Study of Heat Transfer Due to Laminar Flow of Copper–Water Nano Fluid Through Two Isothermally Heated Parallel Plates, International Journal of Thermal Sciences, Vol. 48, No. 2, 2009, pp. 391-400.

[14] Xuan, Y., Li, Q. Heat Transfer Enhancement of Nano Fluids, International Journal of Heat and Fluid Flow, Vol. 21, No. 1, 2000, pp. 58-64.

[15] Kamali, R., Binesh, A. R., Numerical Investigation of Heat Transfer Enhancement Using Carbon Nanotube-Based Non-Newtonian Nano Fluids, International Communications in Heat and Mass Transfer, Vol. 37, No. 8, 2010, pp. 1153-1157.

[16] Jang, S. P., Choi, S. U., Cooling Performance of a Microchannel Heat Sink with Nano Fluids, Applied Thermal Engineering, Vol. 26, No. 17-18, 2006, pp. 2457-2463.

[17] Jung, J. Y., Oh, H. S., and Kwak, H. Y., Forced Convective Heat Transfer of Nanofluids in Microchannels, In Asme 2006 International Mechanical Engineering Congress and Exposition. American Society of Mechanical Engineers, 2006, pp. 327-332,

[18] Koo, J., Kleinstreuer, C., Laminar nanofluid flow in microheat-sinks, International Journal of Heat and Mass Transfer, Vol. 48, No. 13, 2005, pp. 2652-2661.

[19] Madani, K., Numerical Investigation of Cooling a Ribbed Microchannel Using Nanofluid, Journal of Thermal Engineering, Vol. 4, No, 6, 2018, pp. 2408-2422.

[20] Moghari, R. M., Akbarinia, A., Shariat, M., Talebi, F., and Laur, R., Two Phase Mixed Convection Al2O3–Water Nanofluid Flow in an Annulus, International Journal of Multiphase Flow, Vol. 37, No. 6, 2011, pp. 585-595.

[21] Shiriny, A., Bayareh, M., and Nadooshan, A. A., Nanofluid flow in a microchannel with inclined cross-flow injection. SN Applied Sciences, Vol. 1, No. 9, 2019, pp. 1015.

[22] Tsai, T. H., Chein, R., Performance Analysis of Nanofluid-Cooled Microchannel Heat Sinks, International Journal of Heat and Fluid Flow, Vol. 28, No. 5, 2007, pp. 1013-1026.

[23] Bagheri, H., Nadooshan, A. A., The Effects of Hybrid Nano-Powder of Zinc Oxide and Multi Walled Carbon Nanotubes On the Thermal Conductivity of an Antifreeze, Physica E: Low-Dimensional Systems and Nanostructures, Vol. 103, 2018, pp. 361-366.

[24] Abdollahi, A., Mohammed, H. A., Vanaki, S. M., and, Sharma, R. N., Numerical investigation of fluid flow and heat transfer of nanofluids in microchannel with longitudinal fins. Ain Shams Engineering Journal, Vol. 9, No, 4, 2018, pp. 3411-3418.

[25] Ambreen, T., Kim, M. H., Effects of Variable Particle Sizes On Hydrothermal Characteristics of Nanofluids in a Microchannel, International Journal of Heat and Mass Transfer, Vol. 120, 2018, pp. 490-498.

[26] Kahani, M., Simulation of Nano Fluid Flow Through Rectangular Microchannel by Modified Thermal Dispersion Model, Heat Transfer Engineering, 2019, pp. 1-16.

[27] Afrand, M., Karimipour, A., Nadooshan, A. A., and Akbari, M., The Variations of Heat Transfer and Slip Velocity of Fmwnt-Water Nano-Fluid Along the Micro-Channel in The Lack and Presence of a Magnetic Field, Physica E: Low-Dimensional Systems and Nanostructures, Vol. 84, 2016, pp. 474-481.

[28] Nemati, H., Farhadi, M., Sedighi, K., Ashorynejad, H. R., and Fattahi, E. J. S. I., Magnetic Field Effects On Natural Convection Flow of Nano Fluid in A Rectangular Cavity Using the Lattice Boltzmann Model, Scientia Iranica, Vol. 19, No. 2, 2012, pp. 303-310.

[29] Zhao, G., Wang, Z., and Jian, Y., Heat Transfer of the Mhd Nanofluid in Porous Microtubes Under the Electrokinetic Effects, International Journal of Heat and Mass Transfer, Vol. 130, 2019, pp. 821-830.

[30] Jha, B. K., Aina, B., Role of Suction/Injection On Steady Fully Developed Mixed Convection Flow in a Vertical Parallel Plate Microchannel, Ain Shams Engineering Journal, 2016.

[31] Lopez, A., Ibanez, G., Pantoja, J., Moreira, J., and Lastres, O., Entropy Generation Analysis of MHD Nano Fluid Flow in A Porous Vertical Microchannel with Nonlinear Thermal Radiation, Slip Flow and Convective-Radiative Boundary Conditions, International Journal of Heat and Mass Transfer, Vol. 107, 2017, pp. 982-994.

[32] Jalali, E., Karimipour, A., Simulation the Effects of Cross-Flow Injection On the Slip Velocity and Temperature Domain of a Nano Fluid Flow Inside a Microchannel, International Journal of Numerical Methods for Heat & Fluid Flow, Vol. 29, No. 5, 2019, pp. 1546-1562.

[33] Pak, B. C., Cho, Y. I., Hydrodynamic and Heat Transfer Study of Dispersed Fluids with Submicron Metallic Oxide Particles, Experimental Heat Transfer an International Journal, Vol. 11, No. 2, 1998, pp. 151-170.

[34] Buongiorno, J., Convective Transport in Nano Fluids, Journal of Heat Transfer, Vol. 128, No. 3, 2006, pp. 240-250.

[35] Brinkman, H. C., The Viscosity of Concentrated Suspensions and Solutions, The Journal of Chemical Physics, Vol. 20, No. 4, 1952, pp. 571-571.

[36] Patel, H. E., Anoop, K. B., Sundararajan, T., and Das, S. K., A Micro-Convection Model for Thermal Conductivity

of Nano Fluids, In International Heat Transfer Conference
13. Begel House Inc., 2006.